U-Pb dating identifies titanite precipitation in Paleogene sandstones from a volcanic terrane, East Greenland

Rikke Weibel*[1] and Tonny B Thomsen[1]

RESEARCH ARTICLE | OPEN ACCESS
GEUS Bulletin Vol 43 | e2019430203 | Published online: 08 July 2019
https://doi.org/10.34194/GEUSB-201943-02-03

Titanite ($CaTiSiO_5$) occurs as a rare mineral in magmatic and metamorphic rocks. It is commonly found in clastic sedimentary rocks as an accessory heavy mineral – a mineral of high density. Recently, U-Pb dating of single-grains of detrital titanite has been shown to be a useful tool in sedimentary provenance studies (e.g. McAteer *et al*. 2010; Thomsen *et al*. 2015). Titanite U-Pb geochronologies can add important information to constrain the sediment sources of rocks and basins, and can help date precipitation of titanite. However, there are a number of complicating factors that must be taken into consideration for reliable application of titanite U-Pb dating in provenance studies.

First, titanite is less stable than zircon – the most commonly employed dating target. For example, in Palaeocene sediments in the North Sea, titanite rarely occurs as detrital grains at burial depths greater than 1400 m (Morton 1984). It can also show dissolution features due to weathering and burial diagenesis (e.g. Morton 1984; Turner & Morton 2007). Second, titanite may precipitate during burial diagenesis, which would reflect the burial history of sediments and not their provenance. Precipitation of authigenic titanite is documented from deeply buried (i.e. at temperatures greater than 100°C) volcaniclastic sandstones and mudstones (Helmond & Van de Kamp 1984; Milliken 1992) and intrusion-associated mineralisation in volcanic Permian sandstones (van Panhuys-Sigler & Trewin 1990). Moreover, titanite also occurs in shallow-buried Jurassic sandstones with no volcanic affinity (Morad 1988). Thus, the formation of titanite is not necessarily linked to a volcaniclastic source, but nevertheless, the presence of volcanic material seems to promote titanite precipitation. If authigenic titanite precipitation was incorrectly identified as detrital, this would have considerable implications for provenance investigations, as apparently titanite-rich source rocks would be wrongly inferred to be present in the sediment source area. Here, we present examples from the Kangerlussuaq Basin in southern East Greenland of what appeared to be detrital titanite. However, new U-Pb dating reveals that the titanite formed authigenically, and hence contributes to the burial history, and not the provenance, of the sediments.

Geological setting

The Kangerlussuaq Basin in southern East Greenland was formed by the North Atlantic opening during the mid-Cretaceous, and filled by Cretaceous and Palaeogene mud-

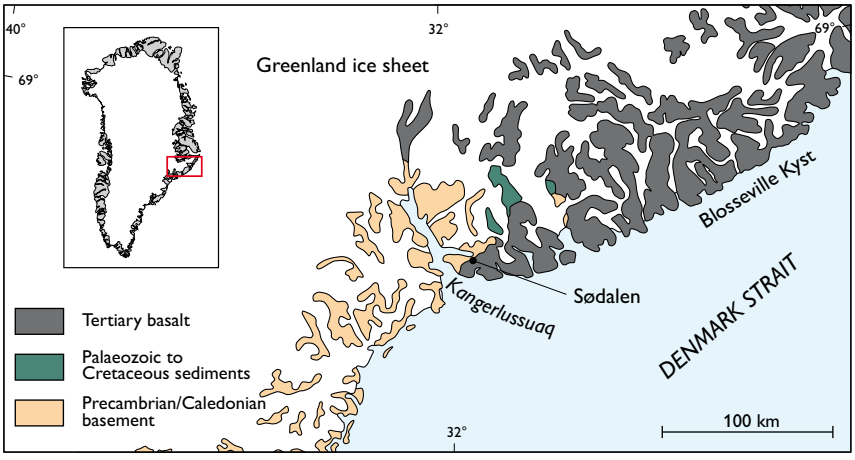

Fig. 1. Distribution of the Palaeozoic to Cretaceous sediments in the Kangerlussuaq area, southern East Greenland, and their close relation to the Tertiary plateau basalt (modified after Henriksen *et al*. 2008).

stone-dominated sediments (Fig. 1; Larsen *et al*. 1999). The type of deposition changed during the Late Cretaceous to sand-prone fluvial deposits (Schjelderup Member), which cover large areas and probably formed due to crustal doming prior to the onset of volcanism (Larsen *et al*. 1999). Several kilometres of Late Palaeocene to Early Eocene continental flood-basalts cover the Cretaceous and Palaeocene sedimentary succession (e.g. Nielsen *et al*. 1981; Peate *et al*. 2003). During breaks in the volcanic activity, siliciclastic deposition resumed in a combination of shallow marine and deltaic environments (Peate *et al*. 2003; Larsen *et al*. 2016). The Kangerlussuaq Basin contains six intrabasaltic sandstone units (Fig. 2; Larsen *et al*. 2016). The earliest intra-basaltic sandstone has the highest content of siliciclastic material, whereas the volcaniclastic contribution increases in the second, and is the main constituent in the succeeding four intrabasaltic sandstone units (Fig. 2).

Methods

The sub- and intra-basaltic sandstones were investigated in thin section by optical microscopy, supplemented by scanning electron microscopy (SEM) of thin sections and rock chips to establish the petrographical and diagenetic relationship between titanite and other mineral phases. A Phillips XL 40 SEM was operated using the secondary electron (SE), back-scattered electron (BSE) and the energy dispersive X-ray spectroscopy (EDS), which combined a Thermo Nanotrace 30 mm^2 detector surface window and a Pioneer Voyager 2.7 10 mm^2 window Si(Li) detector system. The electron beam was generated by a tungsten filament operating at 17 kV and 50–60 μA.

Computer-controlled SEM (CC-SEM) was used for heavy-mineral analysis. Heavy minerals were separated into grains by crushing and ultrasound treatment. The grains were sieved, and the heavy minerals were concentrated from the 45–750 μm fraction by heavy-liquid separation using bromoform. The resulting concentrate was embedded in epoxy and polished. Carbon-coated polished blocks were analysed by SEM under similar conditions as the petrographical investigations. The number of measured grains was typically 1200. The data were recalculated using a method described by Keulen *et al*. (2009). Identification of minerals was based on semi-quantitative EDS (energy dispersive X-ray spectroscopy) analysis, whereby minerals of similar chemical composition were grouped. The mafic silicates include chlorite, amphibole, pyroxene, tourmaline and olivine. The ilmenite group covers altered ilmenite grains with a TiO_2 content of up to 64%, whereas altered grains with a TiO_2 content of 64–90% is considered to be leucoxene. Fragments containing titanite were recorded as titanite only if the composition was TiO_2 > 15%, CaO > 12% and SiO_2 > 15%.

For major- and trace-element analysis, glass discs were produced by fusing ignited powdered samples with lithium tetraborate in Pt/Au crucibles. Most major elements were obtained from the glass discs by X-ray fluorescence (XRF), using a Bruker S8 Tiger wavelength dispersive multichannel XRF spectrometer equipped with a Rh-anode X-ray tube. The elements Na and Cu were acquired by atomic absorption spectrometry (AAS). Trace elements and rare-earth elements were measured by solution-mode inductively coupled plasma mass spectrometry (ICP-MS) using a Perkin Elmer Sciex (Elan 9000) ICP-MS and small pieces of glass disc dissolved in a mixture of HCl and HNO_3.

Titanite U-Pb dating was successfully carried out on one of two samples. The mineral grains were embedded in epoxy mounts and analysed using a NWR213 laser ablation system, coupled to an ELEMENT2 SF-ICP-MS. Titanite grains were hand-picked under a binocular microscope from a heavy mineral concentrate obtained by a Holman–Wilfley water-shaking table. Data were acquired by single-spot analysis bracketed by the GJ-1 zircon standard (Jackson *et al*. 2004).

Results were validated by analyses of natural titanite standards A1772 and A968 (provided by Y. LaHaye), and the Plešovice zircon standard (Slama *et al*. 2008) throughout the analysis sequence, all yielding age accuracies of < 3% (2σ) deviation from reference values. Data processing was performed offline using the software Iolite v. 2.5 (Paton *et al*. 2010, 2011) with the VizualAge data reduction scheme (Petrus & Kamber 2012). Data were corrected for background, session drift and down-hole isotopic fractionation.

A common Pb correction usually needs to be applied for titanites. However, titanites with a high proportion of common Pb, as indicated by low $^{206}Pb/^{204}Pb$ (average *c*. 18 ± 1) and $^{207}Pb/^{204}Pb$ ratios (average *c*. 14 ± 0.5), present a different situation. Ludwig (1998) reports that in such samples, if the common Pb ratio is invariant, any error in the isotope ratios assigned to the common Pb will result in a consistent bias, rather than a random variation, of the calculated $^{206}Pb/^{238}U$ and $^{207}Pb/^{206}Pb$ radiogenic ratios. Thus, in a "SemiTotal–Pb/U isochron" approach (Tera and Wasserburg 1972), the background- and session-drift-corrected ratios can be plotted on the Tera-Wasserburg concordia diagram without correction for common Pb. If (and only if) the true $^{206}Pb/^{238}U$ and $^{207}Pb/^{206}Pb$ radiogenic isotope ratios yield comparable, concordant ages, will the non-common-Pb-corrected data be dispersed along a line whose intercept with the concordia curve defines the age of the samples (Ludwig 1998). This is the case for the titanite grains in this study. Therefore, the

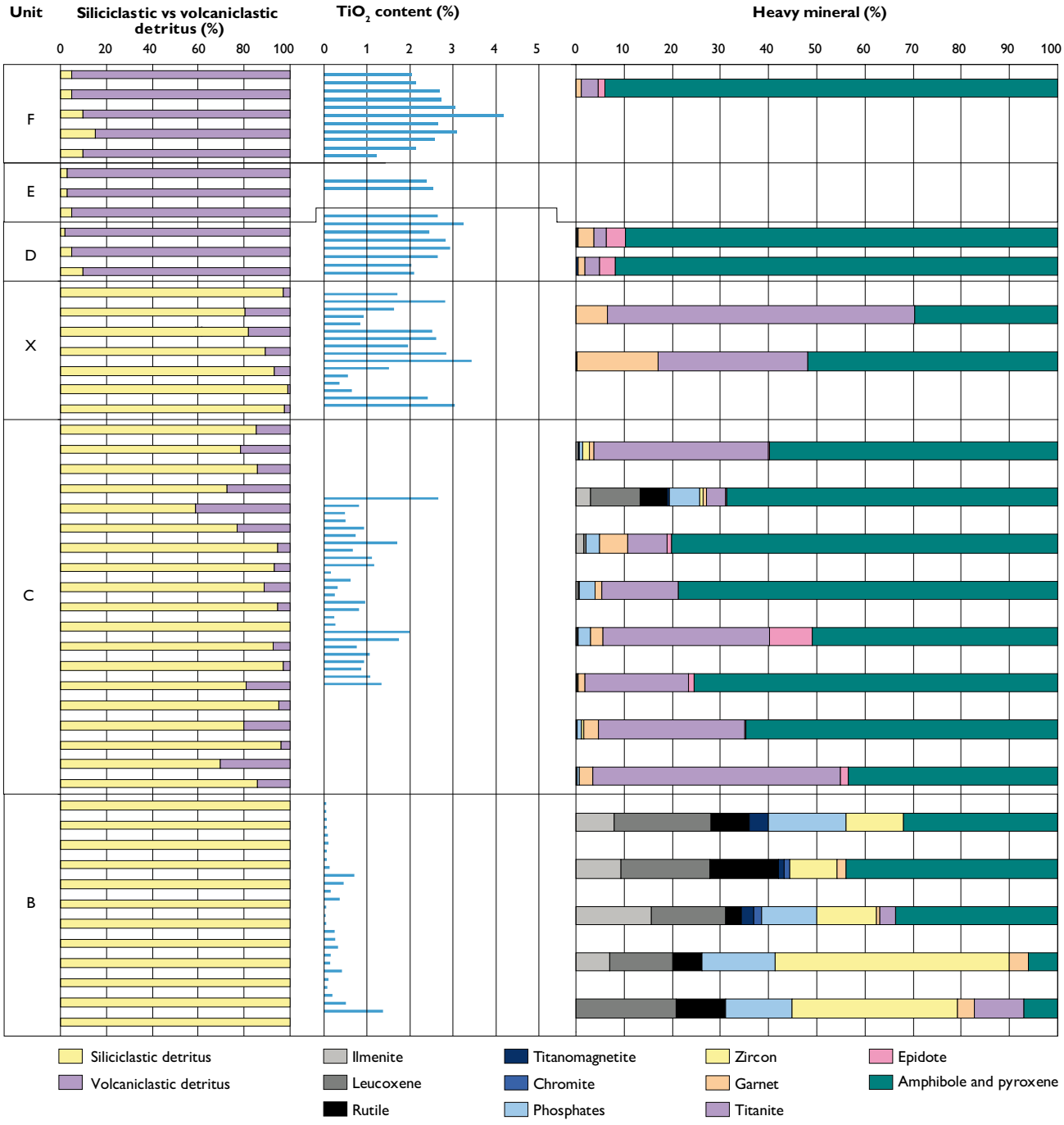

Fig. 2. Bulk rock TiO_2 content and previously published heavy mineral assemblages for sub- and intra-basaltic sandstones (Larsen *et al*. 2016). **Unit B**: sub-basaltic sandstone of the Schjelderup Member. **Units C, X, D, E, F**: intra-basaltic sandstones. Siliciclastic detritus dominates the sub-basaltic sandstones whereas the volcaniclastic content increase upwards. Titanite comprises a relatively large proportion of the heavy minerals in the earliest and second intra-basaltic sandstones, even though the TiO_2 content is even higher in the later intra-basaltic sandstones.

lower intercept age reported here for the titanites is not corrected for common Pb – assuming that the lower intercept age represents the titanite age due to a specific geological event.

Results

The sub- and intra-basaltic sandstones show variations in their detrital grain compositions and exhibit distinctly different cementing phases. The sub-basaltic sandstones consist mainly of quartz, minor amounts of feldspar with subordi-

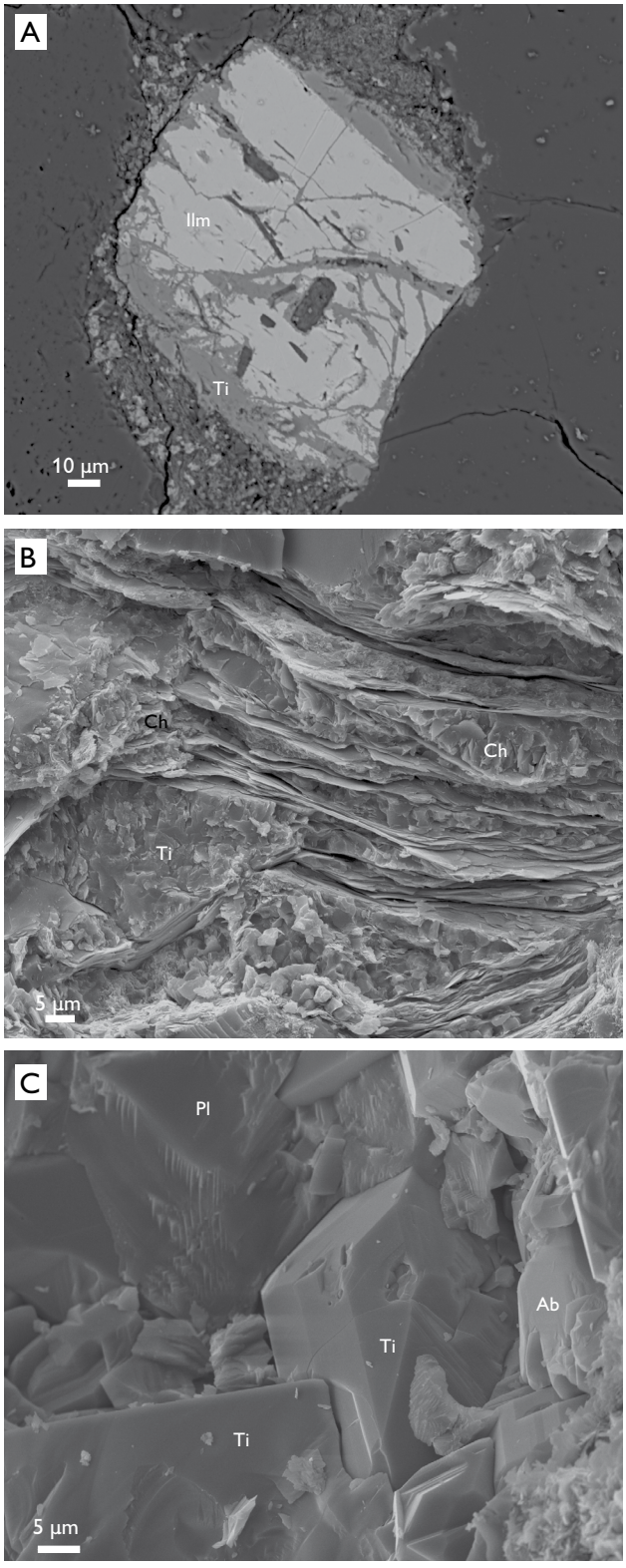

Fig. 3. Micrographs of authigenic titanite. **A**: Titanite (Ti) partially replacing an ilmenite (Ilm) grain (intra-basaltic sandstone; BSE micrograph). **B**: Titanite and chlorite (Ch) precipitated between the cleavage planes in mica (intra-basaltic sandstone; SE micrograph). **C**: Titanite intergrown with albite (Ab) and Ca-rich plagioclase (Pl; intra-basaltic sandstone; SE micrograph).

nate mica, rock fragments and heavy minerals. Besides abundant quartz, the intra-basaltic sandstones are characterised by a high content of detrital feldspar and volcanic rock fragments. The authigenic phases in the sub-basaltic sandstones are dominated by quartz overgrowths and illite. The intra-basaltic sandstones are instead characterised by abundant authigenic chlorite, calcite, common feldspar and rare laumontite cement.

The Ti-rich heavy minerals in the sub-basaltic sandstones are mainly ilmenite, titanomagnetite, leucoxene, rutile and rare titanite (Unit B; Fig. 2). In contrast, titanite is the dominant Ti-rich mineral in the intra-basaltic sandstones. Anatase is the most abundant authigenic phase in the sub-basaltic sandstones, whereas authigenic titanite is dominant in the intra-basaltic sandstones. Titanite commonly occurs as single grains and is a common constituent of rock fragments. Titanite forms tiny crystals together with other authigenic phases such as chlorite and/or calcite, possibly replacing volcanic glass fragments. Authigenic titanite occurs as replacement of detrital ilmenite along fractures and ilmenite crystal rims and as authigenic precipitates, similar to chlorite, between the cleavage planes in mica (Fig. 3).

The bulk rock TiO_2 content increases with abundance of volcaniclastic material, and hence also upwards in the succession of intra-basaltic sandstones (Fig. 2). Although titanite is generally common in the heavy mineral assemblages, it only makes up a relatively small proportion in the volcaniclastic dominated intra-basaltic sandstones, due to more abundant mafic minerals.

The titanite age data are plotted on a Tera-Wasserburg concordia diagram (Fig. 4). The unanchored lower intercept age is reasonably well constrained due to the large spread in radiogenic Pb/common Pb ratios of the titanite grains. In one sample, an analysis of 156 titanite grains yielded a U-Pb lower intercept age of 49 ± 2 Ma (2σ) with a mean square of weighted deviates (MSWD) of 9.6 on both the Tera-Wasserburg and conventional (Wetherill) concordia diagrams.

Discussion

The Ti-rich minerals likely derived from the regional gneiss basement that is assumed to have formed contemporarily with the crystalline basement in the Scoresby Sund region, north of the Kangerlussuaq area, and which yielded U-Pb zircon ages of 2600 to 3000 Ma (Henriksen *et al*. 2008). This is supported by a U-Pb zircon age of 2700–3700 Ma from a Paleogene sandstone in the Kangerlussuaq area (Whitham *et al*. 2004).

Our data show that replacement of ilmenite and titanomagnetite by titanite, and titanite precipitation occurred

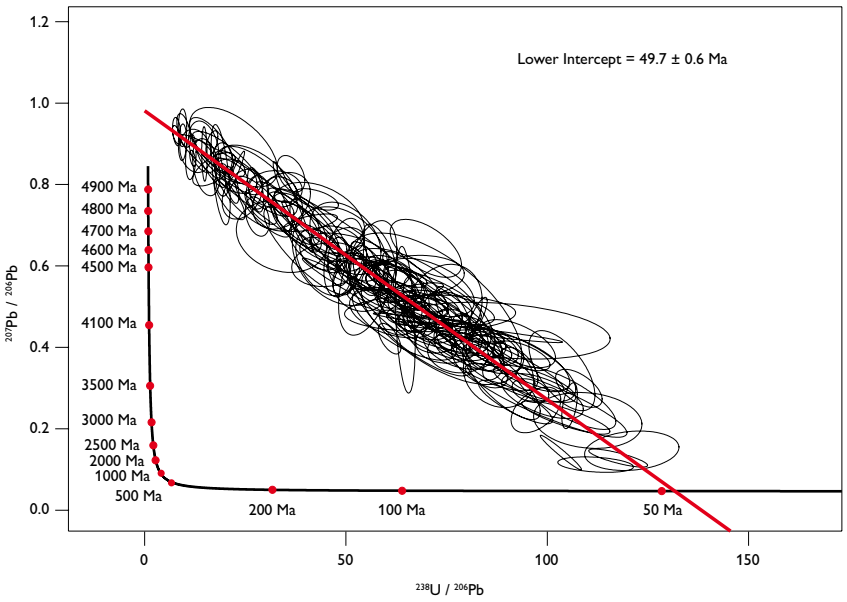

Fig. 4. Tera-Wasserburg diagram. The lower intercept age of *c.* 49 ± 2 Ma calculated for sample 514625 (comprising 158 LA-ICPMS analyses) is indicated. Titanites were not corrected for common Pb content. This age most likely represents titanite precipitation and simultaneous replacement of Fe-Ti oxides during maximum burial due to overlying 56–60 Ma Tertiary flood-basalts.

49–42 Ma (Fig. 4). This probably coincides with maximum burial of the sediments, as thick (6 to 8 km) flood basalt units were extruded over the Kangerlussuaq area with the main eruption phase at 60–50 Ma (Nielsen & Brooks 1981; Larsen & Tegner 2006; Brooks 2011). Furthermore, maximum burial must have occurred prior to the first cooling episode during the Late Eocene (40–35 Ma) as recorded by apatite fission track analyses (Japsen *et al.* 2014).

The reason for preferential precipitation of anatase in sub-basaltic sandstones and titanite in intra-basaltic sandstones, could be that titanite is favoured either by (1) higher temperatures or (2) liberation of Ca and Si simultaneously with alteration of Fe-Ti oxides in intra-basaltic sandstones. The abundance of titanite increases with the volcaniclastic input, hence the fifth and sixth intra-basaltic sandstones (Units F, G; Fig. 2) in the Kangerlussuaq area, which are almost completely dominated by volcaniclastic material, show more abundant titanite than the lower intra-basaltic sandstones, which are comprised of mixed siliciclastic and volcaniclastic material (Units C, X; Fig. 2). Previous investigations show that titanite precipitation is associated with the presence of volcanic rock fragments (Helmond & van de Kamp 1984; van Panhuys-Sigler & Trewin 1990) possibly because Ca, Si and Ti are likely liberated concurrently during alteration of volcanic rock fragments. Formation water from adjacent volcanic rocks could similarly have contributed elements for titanite precipitation. Here, the effect of temperature can be disregarded since the sub- and intrabasaltic sandstones have both experienced similar burial histories of up to 6–8 km burial depth. Alternatively, titanite might have precipitated as a result of the higher heat flux from intrusions or extruded lava, but in this case, a higher abundance of titanite would be expected immediately adjacent to the lava piles or intrusions, which we did not observe.

Conclusions

The sub- and intra-basaltic Paleogene sandstones from the Kangerlussuaq area show a major difference in the dominant Ti-bearing phases. Detrital rutile, ilmenite and leucoxene-replaced Fe-Ti oxides dominate in the sub-basaltic sandstones and anatase is a common authigenic phase. In the intra-basaltic sandstones, titanite is the dominant Ti-phase and here it replaces detrital Ti-rich grains and precipitates as tiny crystals. This reflects different diagenetic changes and not a shift in provenance. U-Pb dating of titanite documents that titanite formed during diagenesis, *c.* 49 Ma, at maximum burial. Despite similar burial history, different diagenetic paths are probably caused by the absence or presence of volcanic material in the sub- and intra-basaltic sandstones, respectively. Seemingly detrital titanite is in fact titanite-replaced Fe-Ti oxides, and hence does not originate from the sediment source area. Care must be taken when working with sediment where abundant volcanic material is present, since it is interpreted to have caused the major difference in dominant Ti-phase between the sub- and intra-basaltic sandstones. The presence of partly titanite-replaced detrital Fe-Ti oxides may indicate that all titanite is authigenic and U-Pb dating may be necessary to establish its true origin.

Acknowledgments

Reviewer Andrew Morton and David Chew are thanked for constructive comments, which improved the paper.

References

Brooks, C. K. 2011: The East Greenland rifted volcanic margin. Geological Survey of Denmark and Greenland Bulletin **24**, 96p.

Helmond, K.P. & van de Kamp, P.C. 1984: Diagenetic mineralogy and controls on albitisation and laumontite formation in Paleogene arkoses, Santa Ynez Mountains, California. In: McDonald, D.A. & Surdam, R.C. (eds): Clastic Diagensis. AAPG Memoir **27**, Tulsa, Oklahoma, 239–276. https://doi.org/10.1306/M37435C15

Henriksen, N., Higgins, A.K., Kalsbeek, F. & Pulvertaft, T.C.R. 2008: Greenland from Archaean to Quaternary. Descriptive text to the 1995 geological map of Greenland. 1:2 500 00. 2nd edition. Geological Survey of Denmark and Greenland Bulletin **18**, 126 pp.

Japsen, P., Green, P.F., Bonow, J.M., Nielsen, T.F.D. & Chalmers, J.A. 2014: From volcanic plains to glaciated peaks: Burial and exhumation history of southern East Greenland after opening of the NE Atlantic. Global and Planetary Change **116**, 91–114. https://doi.org/10.1016/j.gloplacha.2014.01.012

Keulen, N., Hutchison, M.T. & Frei, D. 2009: Computer-controlled scanning electron microscopy: A fast and reliable tool for diamond prospecting. Journal for Geochemical Exploration **103**, 1–5. https://doi.org/10.1016/j.gexplo.2009.04.001

Larsen, R.B. & Tegner, C. 2006: Pressure conditions for the solidification of the Skaergaard intrusion: Eruption of East Greenland flood basalts in less than 300,000 years. Lithos **92**, 181–197. https://doi.org/10.1016/j.lithos.2006.03.032

Larsen, M., Hamberg, L., Olaussen, S., Preuss, T. & Stemmerik, L. 1999: Sandstone wedges of Cretaceous–Lower Tertiary Kangerlussuaq Basin, East Greenland – outcrop analogues to the offshore North Atlantic. In: Fleet, A.J. & Boldy, S.A.R. (eds): Petroleum Geology of Northwest Europe: Proceedings of the 5th Conference, London, 337–348. https://doi.org/10.1144/0050337

Larsen, M., Bell, B., Guarnieri, P., Vosgerau, H. & Weibel, R. 2016: Exploration challenges along the North Atlantic Volcanic Margins – Intrabasaltic sandstone play in subsurface and outcrop. In: Bowman, M. Levell, B. (eds): Petroleum Geology of NW Europe: 50 years of learning. Proceedings of the 8th Petroleum Geology Conference, London: Geological Society, 231–245. https://doi.org/10.1144/pgc8.13

Ludwig, K.R. 1998: On the treatment of concordant uranium-lead ages. Geochimica et Cosmochimica Acta **62**, 4, 665–676. https://doi.org/10.1016/S0016-7037(98)00059-3

McAteer, C.A., Daly, J.S., Flowerdew, M.J., Connelly, J.N., Housh, T.B. & Whitehouse, M.J. 2010: Detrital zircon, detrital titanite and igneous clast U–Pb geochronology and basement–cover relationships of the Colonsay Group, SW Scotland: Laurentian provenance and correlation with the Neoproterozoic Dalradian Supergroup. Precambrian Research **181**, 21–42. https://doi.org/10.1016/j.precamres.2010.05.013

Milliken, K.L. 1992: Chemical behaviour of detrital feldspar in mudrocks versus sandstones, Frio Formation (Oligocene), South Texas. Journal of Sedimentary Research **62**, 790–801. https://doi.org/10.1306/d42679dd-2b26-11d7-8648000102c1865d

Morad, S. 1988: Diagenesis of titaniferous minerals in Jurassic sandstones from the Norwegian Sea. Sedimentary Geology **57**, 17–40. https://doi.org/10.1016/0037-0738(88)90016-4

Morton, A.C. 1984: Stability of detrital heavy minerals in Tertiary sandstones of the North Sea Basin. Clay Minerals **19**, 287–308. https://doi.org/10.1180/claymin.1984.019.3.04

Nielsen, T.F.D. & Brooks, C.K. 1981: The E Greenland rifted continental margin: an examination of the coastal flexure. Journal of Geological Society (London) **138**, 559–568. https://doi.org/10.1144/gsjgs.138.5.0559

Nielsen, T.F.D., Soper, N.J., Brooks, K., Faller, A.M., Higgins, A.C. & Matthews, D.W. 1981: The pre-basaltic sediments and the Lower Basalts at Kangerdlugssuaq, East Greenland: their stratigraphy, lithology, palaeomagnetism and petrology. Meddelelser om Grønland, Geoscience **6**, 3–25.

Paton, C., Woodhead, J.D., Hellstrom, J.C., Hergt, J.M., Greig, A. & Maas, R. 2010: Improved laser ablation U-Pb zircon geochronology through robust downhole fractionation correction. Geochemistry Geophysics Geosystems **11**, 1–36. https://doi.org/10.1029/2009gc002618

Paton, C., Hellstrom, J.C., Paul, P., Woodhead, J.D. & Hergt, J.M. 2011: Iolite: Freeware for the visualisation and processing of mass spectrometric data. Journal of Analytical Atomic Spectrometry **26**, 2508–2518. https://doi.org/10.1039/c1ja10172b

Peate, I.U., Larsen, M. & Lesher, C.E. 2003: The transition from sedimentation to flood volcanism in the Kangerlussuaq Basin, East Greenland: basaltic pyroclastic volcanism during initial Palaeogene continental break-up. Journal of the Geological Society (London) **160**, 759–772. https://doi.org/10.1144/0016-764902-071

Petrus, J.A. & Kamber, B.S. 2012: VizualAge: A novel approach to laser ablation ICP-MS U-Pb geochronology data reduction. Geostandards and Geoanalytical Research **36**, 247–270. https://doi.org/10.1111/j.1751-908x.2012.00158.x

Slama *et al*. 2008. Plešovice zircon — A new natural reference material for U–Pb and Hf isotopic microanalysis. Chemical Geology **249**, 1–35. https://doi.org/10.1016/j.chemgeo.2007.11.005

Tera, F. & Wasserburg, G.J. 1972: U-Th-Pb systematics in three Apollo 14 basalts and the problem of initial lead in lunar rocks. Earth and Planetary Science Letters **14**, 281–304. https://doi.org/10.1016/0012-821x(72)90128-8

Thomsen, T.B., Knudsen, C. & Hinchey, A.M. 2015: Investigations of detrital zircon, rutile and titanite from present-day Labrador drainage basins: fingerprinting the Grenvillean front. Geological Survey of Denmark and Greenland Bulletin **33**, 77–80.

Turner, G. & Morton, A. C. 2007: The effects of burial diagenesis on detrital heavy mineral grain surface textures. In: Mange, M.A. and Wright, D.T. (eds): Heavy minerals in use. Developments in Sedimentology, Elsevier **58**, 393–412. https://doi.org/10.1016/s0070-4571(07)58014-3

Van Panhuys-Sigler, M. & Trewin, N.H. 1990: Authigenic sphene cement in Permian sandstones from Arran. Scottish Journal of Geology **26**, 39–144. https://doi.org/10.1144/sjg26020139

Whitham, A.G., Morton, A.C. & Fanning, C.M. 2004: Insights into Cretaceous–Palaeogene sediment transport paths and basin evolution in the North Atlantic from a heavy mineral study of sandstones from southern East Greenland. Petroleum Geoscience **10**, 61–72. https://doi.org/10.1144/1354-079302-506

How to cite

Weibel, R. & Thomsen, T.B. 2019: U-Pb dating identifies titanite precipitation in Paleogene sandstones from a volcanic terrane, East Greenland. Geological Survey of Denmark and Greenland Bulletin **43**, e2019430203. *https://doi.org/10.34194/GEUSB-201943-02-03*

*Corresponding author: Rikke Weibel | *E-mail: rwh@geus.dk*

[1] *Geological Survey of Denmark and Greenland (GEUS), Øster Voldgade 10, DK-1350, Copenhagen K, Denmark.*